Homolytic C−H Bond Activation by Phosphine−Quinone-Based Radical Ion Pairs

Helling, C.; van der Zee, L.J.C.; Hofman, J.; de Zwart, F.J.; Mathew, S.; Nieger, M.; Slootweg, J.C.

DOI
10.1002/ange.202313397

Publication date
2023

Document Version
Final published version

Published in
Angewandte Chemie

Zitierweise: *Angew. Chem. Int. Ed.* **2023**, *62*, e202313397
doi.org/10.1002/anie.202313397

Radical Ion Pairs | Hot Paper

Homolytic C–H Bond Activation by Phosphine–Quinone-Based Radical Ion Pairs

*Christoph Helling, Lars J. C. van der Zee, Jelle Hofman, Felix J. de Zwart, Simon Mathew, Martin Nieger, and J. Chris Slootweg**

In memory of Edgar Niecke

Abstract: Herein, we present the formation of transient radical ion pairs (RIPs) by single-electron transfer (SET) in phosphine–quinone systems and explore their potential for the activation of C–H bonds. $PMes_3$ (Mes = 2,4,6-$Me_3C_6H_2$) reacts with DDQ (2,3-dichloro-5,6-dicyano-1,4-benzoquinone) with formation of the P–O bonded zwitterionic adduct Mes_3P–DDQ (**1**), while the reaction with the sterically more crowded $PTip_3$ (Tip = 2,4,6-*i*$Pr_3C_6H_2$) afforded C–H bond activation product $Tip_2P(H)$(2-[CMe_2(DDQ)]-4,6-*i*Pr_2-C_6H_2) (**2**). UV/Vis and EPR spectroscopic studies showed that the latter reaction proceeds via initial SET, forming RIP $[PTip_3]^{\bullet+}[DDQ]^{\bullet-}$, and subsequent homolytic C–H bond activation, which was supported by DFT calculations. The isolation of analogous products, $Tip_2P(H)$-(2-[CMe_2{TCQ–$B(C_6F_5)_3$}]-4,6-*i*Pr_2-C_6H_2) (**4**, TCQ = tetrachloro-1,4-benzoquinone) and $Tip_2P(H)$(2-[CMe_2{*o*Q^{tBu}–$B(C_6F_5)_3$}]-4,6-*i*Pr_2-C_6H_2) (**8**, *o*Q^{tBu} = 3,5-di-*tert*-butyl-1,2-benzoquinone), from reactions of $PTip_3$ with Lewis-acid activated quinones, TCQ–$B(C_6F_5)_3$ and *o*Q^{tBu}–$B(C_6F_5)_3$, respectively, further supports the proposed radical mechanism. As such, this study presents key mechanistic insights into the homolytic C–H bond activation by the synergistic action of radical ion pairs.

Electron donor–acceptor systems, like the ubiquitous frustrated Lewis pairs (FLPs), have been widely employed for the activation and functionalization of a plethora of small molecules, including H_2 and CO_2.[1] The common activation mechanism involves polarization of the substrate in the pocket of a weakly associated encounter complex containing both the Lewis acid and Lewis base components, which induces heterolytic bond cleavage via polar, two-electron processes.[2] In contrast, recent studies have shown that radical species are accessible from closed-shell FLP systems by single-electron transfer (SET), which offers the potential for the complementary homolytic bond activation of substrates.[3] This is particularly appealing for the rather inert and difficult to polarize C–H bonds.[4] Indeed, the design and development of suitable radical pathways of FLP-derived systems for the selective activation of C–H bonds is highly desirable, yet only limited examples are reported to date. The first example is reported by Stephan and co-workers, who observed the formation of $[Nap_3PR]$-$[(\mu\text{-OH})(Al(C_6F_5)_3)_2]$ (**B**) (Nap = 1-naphthyl; R = CH_2Ph, C_6H_4Br), when exposing a 1:2 mixture of Nap_3P and $Al(C_6F_5)_3$ to N_2O in either toluene or bromobenzene, and explained its formation via homolytic C–H bond activation of the solvent by the transient radical ion pair (RIP) $[Nap_3P]^{\bullet+}[(\mu\text{-O})(Al(C_6F_5)_3)_2]^{\bullet-}$ (**A**) (Scheme 1a).[5] This

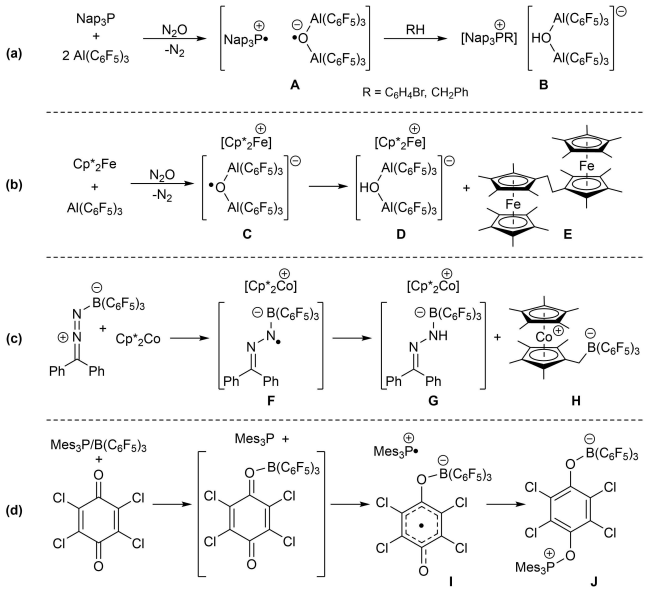

Scheme 1. C–H bond activation by (a) a transient *in situ* generated RIP, (b) an *O*-centred radical anion, and (c) a *N*-centred radical anion. (d) Reactivity of the FLP $Mes_3P/B(C_6F_5)_3$ towards TCQ.

[*] Dr. C. Helling, L. J. C. van der Zee, J. Hofman, F. J. de Zwart, Dr. S. Mathew, Assoc. Prof. Dr. J. C. Slootweg
Van't Hoff Institute for Molecular Sciences, University of Amsterdam,
PO Box 94157, 1090 GD Amsterdam (The Netherlands)
E-mail: j.c.slootweg@uva.nl
Dr. M. Nieger
Department of Chemistry, University of Helsinki,
A. I. Virtasen aukio 1, P.O. Box 55, FIN-00014 Helsinki (Finland)

finding was supported by the characterisation of the phosphine radical cation $[Mes_3P]^{\bullet+}$ when using Mes_3P (Mes = 2,4,6-$Me_3C_6H_2$). Our calculations confirm that thermal SET is only feasible from the phosphine donor towards N_2O when two equivalents of $Al(C_6F_5)_3$ are coordinated (electron affinity (EA) increases from −2.07 eV for N_2O to −4.97 eV for $(\mu\text{-}ON_2)(Al(C_6F_5)_3)_2$).[6] Similarly, when using metallocenes as single-electron donors, Severin et al. showed that the putative oxyl radical anion in $[Cp^*_2Fe]^+[(\mu\text{-}O)(Al(C_6F_5)_3)_2]^{\bullet-}$ (**C**, $Cp^* = C_5Me_5$) is able to effect C–H bond activation of the cyclopentadienyl methyl-substituent forming $[Cp^*_2Fe][(\mu\text{-}OH)(Al(C_6F_5)_3)_2]$ (**D**) and Cp^*_2Fe-derived dimer **E** (Scheme 1b).[7] Using the more potent metallocene electron donor Cp^*_2Co and the thermally unstable diazomethane–borane adduct $Ph_2CNN–B(C_6F_5)_3$, Stephan et al. postulated single-electron transfer to occur generating the transient radical ion pair $[Cp^*_2Co]^+[Ph_2CNN–B(C_6F_5)_3]^{\bullet-}$ (**F**), which undergoes an analogous hydrogen atom abstraction reaction forming $[Cp^*_2Co][Ph_2CNN(H)B(C_6F_5)_3]$ (**G**) and the cobaltocene C–H activated species (**H**) (Scheme 1c);[8] only when using 9-diazofluorene and $Al(C_6F_5)_3$ the corresponding radical anion $[(C_{12}H_8)CNN–Al(C_6F_5)_3]^{\bullet-}$ could be detected by EPR spectroscopy.[8] In these studies, the postulated radical ion pair intermediates were not observed spectroscopically, and the radical nature of the C–H bond activations was thus only supported by detection of the above mentioned paramagnetic species.[9] Moreover, SET reactions between N-heterocyclic carbenes and triarylcarbenium ions as electron acceptors resulted in C–H bond activations due to the highly reactive nature of carbene-derived radical cations.[10]

In a seminal study, Stephan and co-workers treated the FLP system $Mes_3P/E(C_6F_5)_3$ (E = B, Al) with the tetrachloro-1,4-benzoquinone (TCQ) electron acceptor and obtained the zwitterionic adduct $[Mes_3POC_6Cl_4OE(C_6F_5)_3]$ (**J**);[3c] only the $Mes_3P^{\bullet+}$ radical cation intermediate was observed by EPR spectroscopy. Subsequent mechanistic investigations from our group revealed that this reaction proceeds via thermally-induced SET[11] from $PMes_3$ to the Lewis acid-activated substrate $TCQ–B(C_6F_5)_3$ affording the transient RIP $[Mes_3P]^{\bullet+}[TCQ–B(C_6F_5)_3]^{\bullet-}$ (**I**), which subsequently undergoes radical coupling by P–O bond formation to afford **J** (Scheme 1d).[12] Based on these studies, we reasoned that steric frustration in phosphine–quinone systems offers the potential for the detection of reactive RIPs by thermal SET. Herein, we report on the steric and electronic factors influencing the formation of transient RIPs, generated by SET from sterically demanding triarylphosphines to (Lewis acid-activated) quinones, and investigate their potential for C–H bond activation reactivity.

First, we set out to explore the redox chemistry of bulky triarylphosphine electron donors $PMes_3$ (ionization energy (IE) = 5.16 eV) and $PTip_3$ (IE = 4.83 eV; Tip = 2,4,6-$iPr_3C_6H_2$) with the strongly oxidizing quinone 2,3-dichloro-5,6-dicyano-1,4-benzoquinone (DDQ; EA = −5.18 eV), as our DFT calculations at the SCRF(DCM)/(U)ωB97X–D/6-311 + G(d,p)//(U)ωB97X-D/6-31G(d) level of theory indicate thermal SET to be feasible ($\Delta E = -0.02$ eV and −0.35 eV, respectively). Treatment of $PMes_3$ with DDQ in DCM at ambient temperature resulted directly in a light brown solution, which after work-up afforded **1** (84 %, $\delta^{31}P\{^1H\} = 70.7$ ppm; Scheme 2) as a yellow crystalline solid. Single-crystal X-ray diffraction analysis unequivocally established the formation of a 1:1 adduct, $Mes_3P–DDQ$ (Scheme 2).[13] Electron donor–acceptor adduct **1**, with its P–O bond length of 1.6030(10) Å and typical metrics for a reduced DDQ moiety,[14] is structurally similar to Stephan's compound **J** (P–O 1.606(3) Å, $\delta^{31}P\{^1H\} = 70.8$ ppm),[3c] yet due to the increased electron accepting capability of DDQ no Lewis acid activation is required (cf. EA(TCQ) = −4.55 eV, $EA(TCQ–B(C_6F_5)_3) = -5.61$ eV). *In situ* NMR, EPR and UV/Vis spectroscopic studies yielded no definite proof for radical ion pair intermediates, apart from a weak EPR signal assigned to $[DDQ]^{\bullet-}$ next to an unidentified radical in a flash frozen solution (Figure S49), as well as UV/Vis spectroscopic indications for the presence of $[DDQ]^{\bullet-}$ ($\lambda_{max} = 461$, 547, and 587 nm; Figure S50).[15] **1** is thermally stable, both in the solid state and in solution, and a reversible dissociation into the corresponding RIP $[Mes_3P]^{\bullet+}[DDQ]^{\bullet-}$ by homolytic P–O bond cleavage, even at elevated temperatures (100 °C), was not observed.

Next, in an attempt to prevent P–O adduct formation, we resorted to the sterically more encumbered and stronger electron-donating phosphine $PTip_3$.[16] Interestingly, dissolving a solid mixture of $PTip_3$ and DDQ in DCM at ambient temperature afforded immediately an intense deep purple colour that quickly decolourized in minutes yielding a red solution, which after work-up provided **2** as yellow crystals

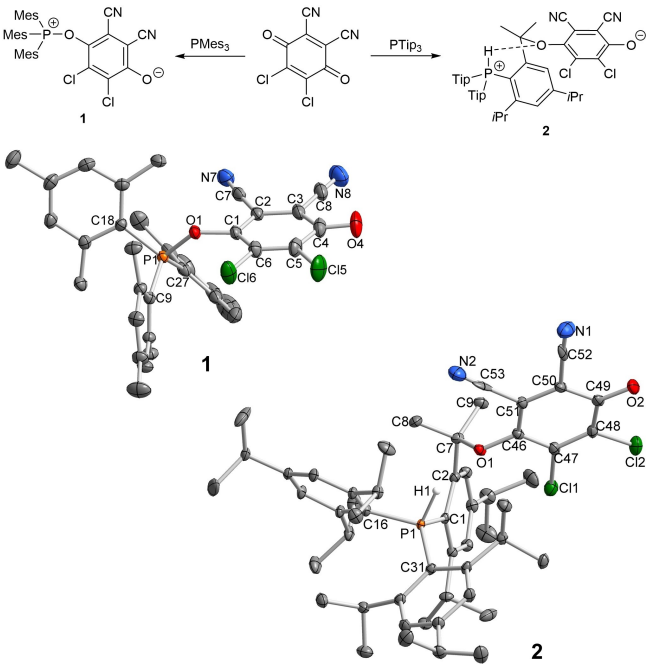

Scheme 2. Synthesis of compounds **1** and **2** (top) and molecular structures of **1** and **2** (bottom). Hydrogen atoms (except P–H in **2**) and co-crystallized molecule of chlorobenzene (**1**) were omitted for clarity. Displacement ellipsoids are drawn at 50% probability level. Selected bond lengths [Å] for **1**: P1–O1 1.6030(1). **2**: P1–H1 1.34(3), O1···H1 2.011(5), C7–O1 1.491(3).

(85 %; Scheme 2). ^{1}H and ^{31}P NMR spectroscopic analysis revealed **2** to be diamagnetic with a distinctly different ^{31}P chemical shift ($\delta^{31}P = -28.7$ ppm) than **1**, the presence of a P–H moiety ($\delta^{1}H = 9.74$ ppm, $^{1}J_{HP} = 510.5$ Hz) and inequivalent $CH(CH_3)_2$ resonances, indicative of C–H bond activation of a single *i*Pr group. Indeed, the molecular structure of the zwitterionic $Tip_2P(H)(2\text{-}[CMe_2(DDQ)]\text{-}4,6\text{-}iPr_2\text{-}C_6H_2)$ **2** in the solid state (Scheme 2)[13] confirmed C–H bond activation of an *ortho*-*i*Pr group and its connection to the quinone moiety via the newly formed C7–O1 bond (1.491(3) Å).[17] Interestingly, there is a short P–H···O contact between the hydrophosphonium and hydroquinone moiety via hydrogen bonding (P1–H1 1.34(3) Å, O1···H1 2.011(5) Å). Although at ambient temperature **2** is thermally stable in the solid-state, freshly prepared, yellow solutions of **2** in DCM decompose with colour change to red and formation of free $PTip_3$ and $DDQ^{\bullet-}$ as well as another unidentified species ($\delta^{31}P\{^{1}H\} = 19.8$ ppm) as detected by NMR, UV/Vis and EPR spectroscopy (Figures S54–56), indicating a potential reversibility of the reaction.

To shed light on the origin of the deep purple colour that could be indicative for the formation of the RIP $[Tip_3P]^{\bullet+}[DDQ]^{\bullet-}$, we resorted again to *in situ* EPR and UV/Vis spectroscopy. Indeed, X-band EPR analysis at 170 K of a flash frozen sample of the reaction mixture taken immediately after addition of DCM to solid $PTip_3$ and DDQ confirmed the formation of $PTip_3^{\bullet+}$ (axial four-line signal simulated with $S = 1/2$, $g_{\perp} = 2.0060$, $g_{\parallel} = 2.0016$, $a^{31P}{}_{\perp} = 381.2$ MHz, $a^{31P}{}_{\parallel} = 1168.4$ MHz),[18] but also showed a small signal ($S = 1/2$, $g_{iso} = 2.0049$) that we attribute to $[DDQ]^{\bullet-}$ (Figure 1a, Figure S53). The low EPR signal intensity of $[DDQ]^{\bullet-}$ is likely due to aggregation to the corresponding $[DDQ]_2^{2-}$ dimer at low temperature as observed by Kochi et al.[15] Ambient temperature UV/Vis spectroscopy supports the formation of RIP $[Tip_3P]^{\bullet+}[DDQ]^{\bullet-}$ as it clearly shows the presence of $[DDQ]^{\bullet-}$ in the reaction mixture ($\lambda = 461$, 540 and 584 nm; Figure 1b),[15] as well as a broad, low-intensity absorption band ($\lambda_{max} = 713$ nm) indicative of the dimer $[DDQ]_2^{2-}$.[15] The phosphoniumyl radical cation $[PTip_3]^{\bullet+}$ could not be unambiguously identified due to its broad absorption at $\lambda_{max} = 525$ nm,[18] which is obscured by the intense absorptions of $[DDQ]^{\bullet-}$. Unfortunately, due to the short-lived nature of RIP $[Tip_3P]^{\bullet+}[DDQ]^{\bullet-}$, crystallization attempts were unsuccessful.

To further support the experimental observation of RIP $[Tip_3P]^{\bullet+}[DDQ]^{\bullet-}$ and investigate its role in the formation of the C–H bond-activated **2**, we performed calculations at the SCRF(DCM)/(U)ωB97X–D/6-311+G-(d,p)//(U)ωB97X–D/6-31G(d) level of theory (Figure 2). According to these calculations, $PTip_3$ and DDQ form an electron donor–acceptor (EDA) complex $[PTip_3,DDQ]$ ($\Delta G = 5.1$ kcal·mol^{-1}) via a slightly endergonic process, after which SET affords the thermodynamically favoured open-shell singlet RIP $^{1}\{[Tip_3P]^{\bullet+}[DDQ]^{\bullet-}\}$ ($\Delta G = -8.7$ kcal·mol^{-1}). Intersystem crossing (ISC) may afford triplet RIP $^{3}\{[Tip_3P]^{\bullet+}[DDQ]^{\bullet-}\}$ ($\Delta G = -9.3$ kcal·mol^{-1}) and subsequent dissociation gives the separate $[PTip_3]^{\bullet+}$ and $[DDQ]^{\bullet-}$ radicals ($\Delta G = -12.1$ kcal·mol^{-1}). Alternatively, the open-shell singlet $^{1}\{[Tip_3P]^{\bullet+}[DDQ]^{\bullet-}\}$ can directly

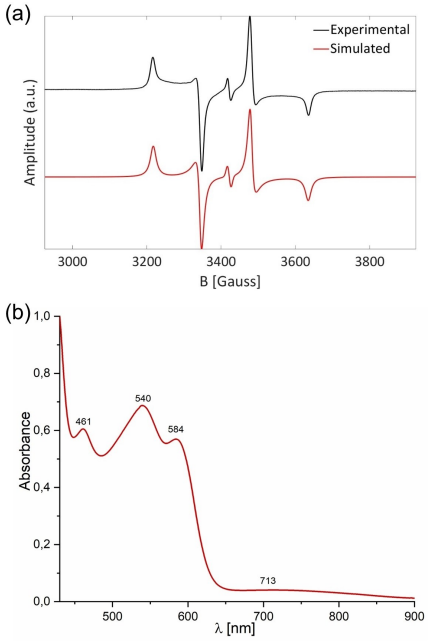

Figure 1. (a) X-band EPR spectrum (170 K) of a flash frozen reaction mixture of $PTip_3$ and DDQ in DCM. [Experimental details: microwave frequency = 9.642632 GHz, power = 0.6325 mW, modulation amplitude = 1.000 G. Simulation parameters: $[PTip_3]^{\bullet+}$: $S = 1/2$, $g_{\perp} = 2.0060$, $g_{\parallel} = 2.0016$, lwpp = 1.11 mT (Lorentzian), $a^{31P}{}_{\perp} = 381$ MHz, $a^{31P}{}_{\parallel} = 1168$ MHz; $[DDQ]^{\bullet-}$: $S = 1/2$, $g_{iso} = 2.0049$, lwpp = 1.01 mT (Gaussian); ratio $[PTip_3]^{\bullet+}$: $[DDQ]^{\bullet-} = 1.0 : 0.0037$]. (b) UV/Vis spectrum of the initial reaction mixture of $PTip_3$ and DDQ in DCM.

engage in homolytic C–H bond activation. This process proceeds via hydrogen atom transfer of the *ortho*-$CH(CH_3)_2$ atom from carbon to phosphorus (**TS1$_{OS}$**; $\Delta G^{\ddagger} = 19.3$ kcal·mol^{-1}) and affords the fleeting hydrophosphonium RIP intermediate **INT** ($\Delta G = 7.6$ kcal·mol^{-1}). Subsequent radical coupling with C–O bond formation (**TS2$_{OS}$**; $\Delta G^{\ddagger} = 5.8$ kcal·mol^{-1}) furnishes a rotamer of product **2** (**2$_{rot}$**, $\Delta G = -7.7$ kcal·mol^{-1}), which is of comparable stability as RIP $^{1}\{[Tip_3P]^{\bullet+}[DDQ]^{\bullet-}\}$ underlining its thermal lability. Rotation about the C_{Ar}–CMe_2(DDQ) bond to establish the O···H contact observed in the X-ray structure yields compound **2**, which was calculated to be 6.1 kcal·mol^{-1} and 14.8 kcal·mol^{-1} lower in energy compared to $^{1}\{[Tip_3P]^{\bullet+}[DDQ]^{\bullet-}\}$ and the starting materials, respectively. Since $[PTip_3]^{\bullet+}$ is thermally indefinitely stable,[18,19] our findings fully support the cooperative action of both $[PTip_3]^{\bullet+}$ and $[DDQ]^{\bullet-}$ in the facile formation of **2** by homolytic (radical) C–H bond activation. Contrastingly, a high-energy, two-electron pathway connecting EDA complex $[PTip_3,DDQ]$ directly with **2** was also found, yet the calculated barrier (**TS1$_{CS}$**; $\Delta G^{\ddagger} = 37.3$ kcal·mol^{-1}) contradicts the experimental reaction conditions (20 °C, $t < 10$ min).

To prove the generality of the cooperative homolytic C–H bond activation between $PTip_3$ and quinones, we focussed on using other quinones as electron acceptors. As observed for $PMes_3$,[3c] no direct reaction between $PTip_3$ and TCQ (EA = −4.55 eV) in DCM was detected, even at 50 °C, which supports the relevance of matching electron donating

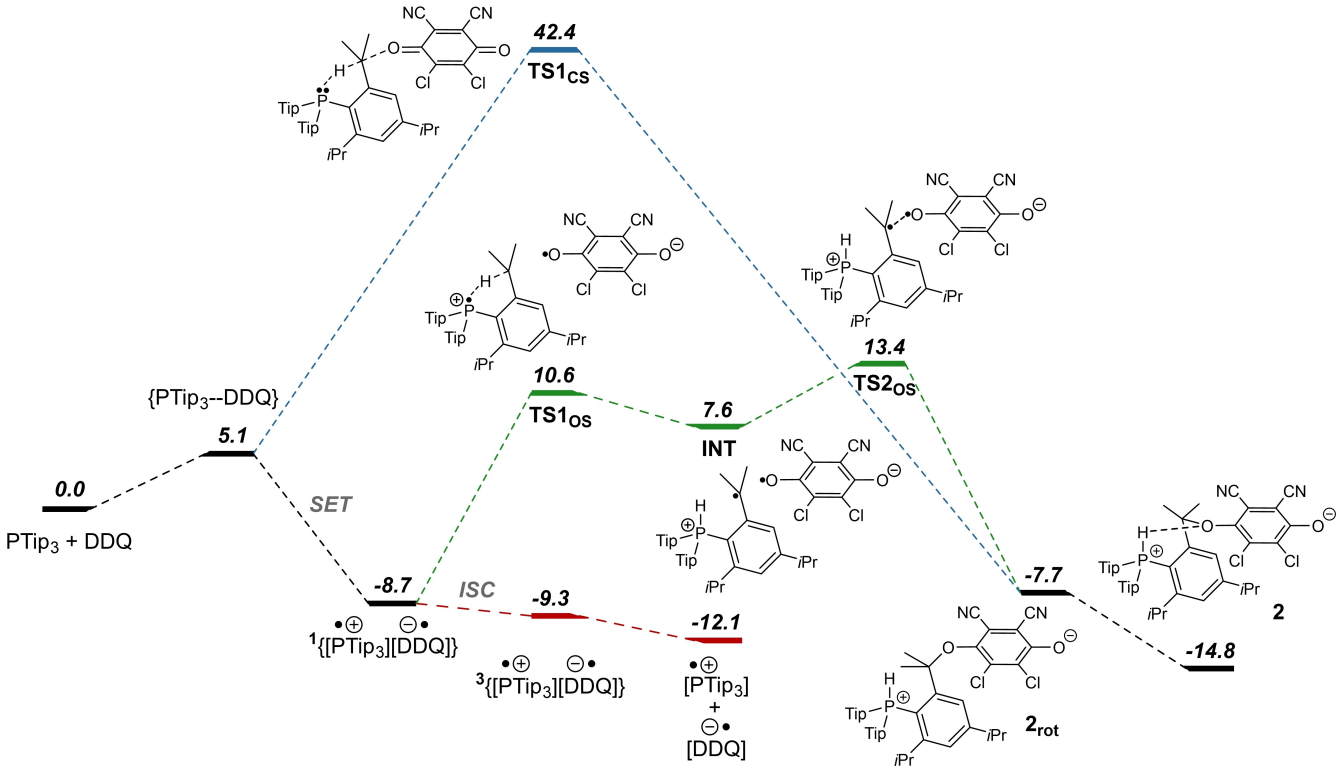

Figure 2. Computed relative Gibbs free energies ΔG (SCRF(DCM)//(U)ωB97X–D/6–311+G(d,p)//(U)ωB97X–D/6–31G(d); in kcal·mol^{-1}) for closed-shell and open-shell pathways for the formation of **2** from $PTip_3$ and DDQ.

and accepting capabilities of phosphine and quinone, respectively. On the other hand, in the presence of one equivalent of $B(C_6F_5)_3$ (EA(TCQ–$B(C_6F_5)_3$) = −5.61 eV), upon mixing TCQ with $PTip_3$, immediately a persisting deep red colour was obtained at ambient temperature. After work-up, thermally stable deep red crystals of **3** (69 %; Scheme 3) were obtained from chlorobenzene that were ^{31}P NMR silent. Indeed, the molecular structure of **3** in the crystal confirmed the formation of the paramagnetic phosphoniumyl radical salt $[PTip_3]^{\bullet+}{}_2[(F_5C_6)_3BOC_6Cl_4OB(C_6F_5)_3]^{2-}$ (**3**; Figure S67);[13] its structural features of the $[PTip_3]^{\bullet+}$ radical cation and the $[(F_5C_6)_3BOC_6Cl_4OB(C_6F_5)_3]^{2-}$ dianion are similar to those previously reported.[3c,e,18] Since only 0.5 equivalents of TCQ is incorporated in **3**, we also performed the reaction of equimolar amounts of $PTip_3$, TCQ and $B(C_6F_5)_3$ in DCM at 50 °C. Interestingly, a gradual decolouration of the deep red solution was observed yielding a colourless solution after 7 days, from which **4** was obtained as colourless crystals (59 %; $\delta^{31}P = -28.5$ ppm, $^1J_{PH} = 507.8$ Hz; Scheme 3). Its molecular structure firmly established **4** being the C–H bond activation product $Tip_2P(H)$(2-[CMe_2{TCQ–B$(C_6F_5)_3$}]-4,6-*i*Pr_2-C_6H_2) (Scheme 3),[13] structurally analogous to **2**. The formation of **4** indicates that under the reaction conditions small amounts of the radical ion pair $[Tip_3P]^{\bullet+}$ [TCQ–$B(C_6F_5)_3]^{\bullet-}$ are available that can undergo C–H bond activation similar to $[Tip_3P]^{\bullet+}[DDQ]^{\bullet-}$.

Next, we reasoned that by using sterically more demanding quinones, the persistency of the RIP intermediates could

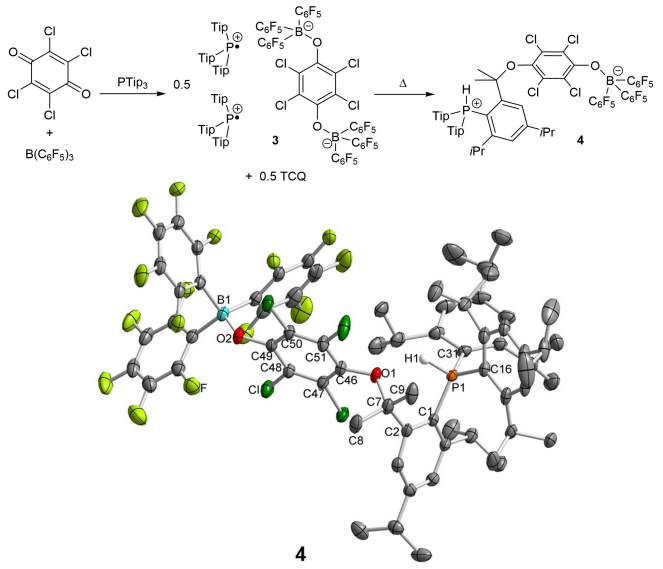

Scheme 3. Synthesis of compounds **3** and **4** (top) and molecular structure of **4** (bottom). Hydrogen atoms (except P–H) were omitted for clarity. Displacement ellipsoids are drawn at 50 % probability level. Selected bond lengths [Å] for **4**: P1–H1 1.32(2), C7–O1 1.482(3), O2–B1 1.508(3).

be improved by suppressing the P–O adduct formation or C–H activation. For this, we selected the commercially available *t*Bu-substituted quinones 2,6-di-*tert*-butyl-1,4-benzoquinone (pQ^{tBu}; EA = −3.63 eV) and 3,5-di-*tert*-butyl-1,2-

benzoquinone (oQ^{tBu}; EA = −3.81 eV). To enhance their electron affinity, $B(C_6F_5)_3$ was used as activator (EA-(pQ^{tBu}–$B(C_6F_5)_3$ (**5**)) = −4.74 eV; EA(oQ^{tBu}–$B(C_6F_5)_3$ (**6**)) = −4.81 eV) to facilitate thermal SET.[20] Both Lewis acid-activated quinones pQ^{tBu}–$B(C_6F_5)_3$ (**5**; 71 %; $\delta^{11}B = 5.5$ ppm) and oQ^{tBu}–$B(C_6F_5)_3$ (**6**; 70 %; $\delta^{11}B = 11.1$ ppm) were obtained simply by mixing the quinone with one equivalent of $B(C_6F_5)_3$ in toluene and isolated as dark red crystalline solids. The molecular structures of **5** and **6** in the crystal reveal that the quinones coordinate to the borane via the less sterically shielded oxygen centres in the 4-position and 1-position, respectively (Figure 3).[13]

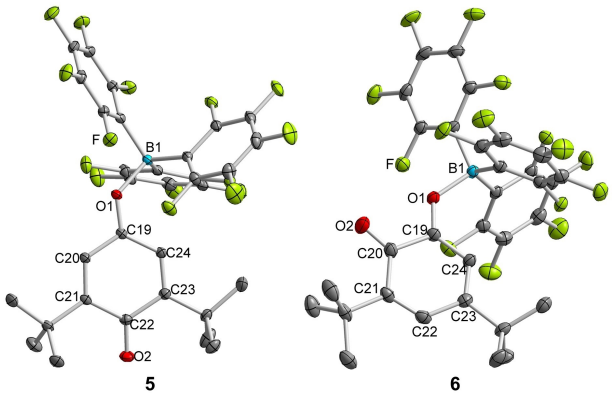

Figure 3. Molecular structures of **5** and **6**. Hydrogen atoms and co-crystallized molecule of toluene (**5**) were omitted for clarity. Displacement ellipsoids are drawn at 50% probability level. Selected bond lengths [Å] for **5**: B1–O1 1.5762(14); **6**: B1–O1 1.571(2).

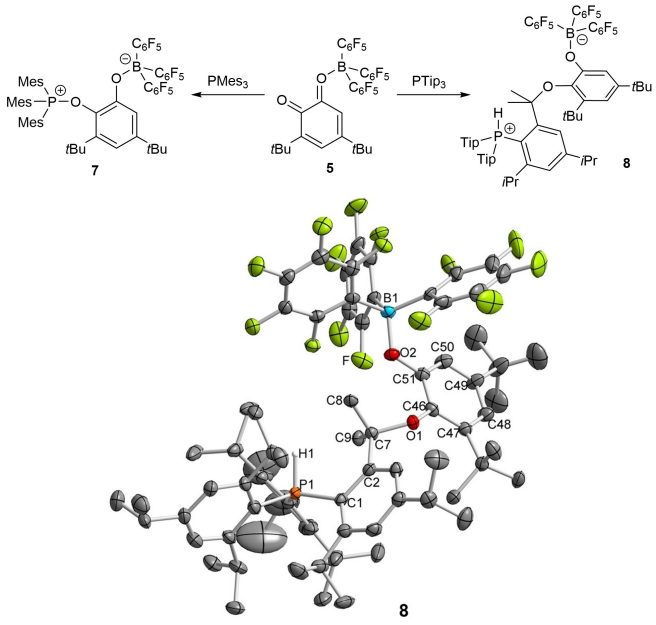

Scheme 4. Synthesis of compounds **7** and **8** (top) and molecular structure of **8** (bottom). Hydrogen atoms (except P–H) were omitted for clarity. Displacement ellipsoids are drawn at 50% probability level. Selected bond lengths [Å] for **8**: P1–H1 1.37(3), C7–O1 1.492(5), O2–B1 1.500(6).

Upon mixing $PMes_3$ with *para*-quinone adduct **5** in DCM no colour changes indicative of potential SET processes were observed; indeed our DFT calculations indicate for this system thermal SET to be unlikely ($\Delta E = 0.42$ eV). Instead, combining $PTip_3$ with **5** in DCM gave rise to an instant colour change from orange to bright red indicative for SET and formation of RIP $[PTip_3]^{\bullet+}[pQ^{tBu}–B(C_6F_5)_3]^{\bullet-}$. EPR spectroscopy confirmed the presence of $[PTip_3]^{\bullet+}$ ($S = 1/2$, $g = 2.0053$, $a^{31P}_{iso} = 662.8$ MHz; Figure S64)[3e,18] and also displayed a featureless signal at $g = 2.0039$ with very low intensity that we attributed to the semiquinone radical anion $[pQ^{tBu}–B(C_6F_5)_3]^{\bullet-}$. However, C–H bond activation was not observed, likely due to effective shielding of the quinone O centre by the adjacent *t*Bu groups. *Ortho*-quinone adduct **6** proved to be more reactive. The addition of $PMes_3$ to **6** afforded colourless crystals of electron donor–acceptor adduct $[Mes_3P–oQ^{tBu}–B(C_6F_5)_3]$ (**7**, 72 %, $\delta^{31}P\{^1H\} = 69.1$ ppm; Scheme 4; Figure S68).[13] No colour changes have been observed, which is in accordance with the relatively large energy barrier for SET ($\Delta E = 0.35$ eV). In contrast, $PTip_3$ again induced SET to give a deep purple solution that is persistent for hours. X-band EPR spectroscopy at ambient temperatures clearly featured signals attributable to both radicals of the RIP $[PTip_3]^{\bullet+}[oQ^{tBu}–B(C_6F_5)_3]^{\bullet-}$, *i.e.*, a broad doublet for $[PTip_3]^{\bullet+}$ ($S = 1/2$, $g_{iso} = 2.0057$, $a^{31P}_{iso} = 661.4$ MHz),[3e,18] and a featureless singlet ($S = 1/2$, $g = 2.0038$) assigned to radical anion $[oQ^{tBu}–B(C_6F_5)_3]^{\bullet-}$ (Figure 4).

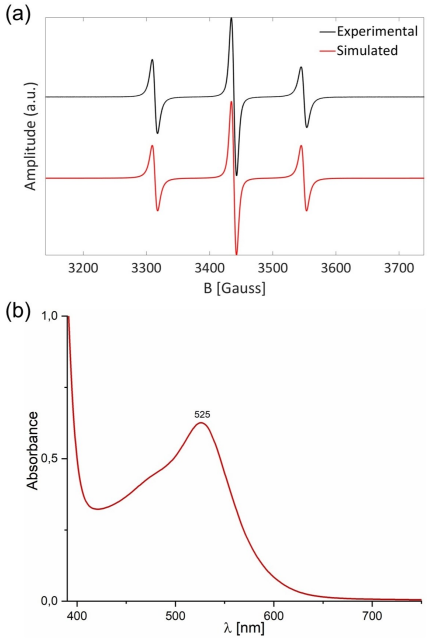

Figure 4. (a) X-band EPR spectrum (RT) of the reaction mixture of $PTip_3$ and **5** in DCM. [Experimental parameters: microwave frequency: 9.643661 GHz, power: 6.325 mW, Modulation amplitude: 1.000 G; Simulation parameters: $[PTip_3]^{\bullet+}$: $S = 1/2$, $g_{iso} = 2.0057$, $a^{31P}_{iso} = 661$ MHz, lwpp = 0.301 mT & 0.741 mT (Gaussian & Lorentzian); $[\mathbf{5}]^{\bullet-}$: $S = 1/2$, $g_{iso} = 2.0038$, lwpp = 0.559 mT & 0.423 mT (Gaussian & Lorentzian); ratio $[PTip_3]^{\bullet+}$: $[\mathbf{5}]^{\bullet-} = 1.0 : 0.64$.]. (b) UV/Vis spectrum of the reaction mixture of $PTip_3$ and **5** in DCM.

Work-up after 24 hours afforded colourless crystals of C–H activated product $Tip_2P(H)(2\text{-}[CMe_2\{oQ^{tBu}\text{–}B(C_6F_5)_3\}]\text{-}4,6\text{-}i Pr_2\text{-}C_6H_2)$ (**8**) (45 %, $\delta^{31}P = -27.1$ ppm, $^1J_{PH} = 476.5$ Hz; Scheme 4), whereas attempts to crystallize the intermediate RIP $[PTip_3]^{\bullet+}[oQ^{tBu}\text{–}B(C_6F_5)_3]^{\bullet-}$ have been unsuccessful. The molecular structure of **8** was unambiguously established by single crystal X-ray analysis and shows similar features as **2** and **4** (Scheme 4),[13] which highlights the generality of the homolytic C–H bond activation of $PTip_3$ when using structurally different yet similarly electron accepting quinones.

In summary, we demonstrated that phosphine donors react in different ways with quinone-based electron acceptors. While $PMes_3$ afforded 1:1 electron donor-acceptor adducts, exemplified by the isolation of **1** and **7**, the bulkier and more electron donating $PTip_3$ induced thermal SET affording radical ion pairs that could be spectroscopically characterised. Mechanistic insight into the subsequent cooperative homolytic (radical) C–H bond activation leading to zwitterions **2**, **4**, and **8** was provided by DFT calculations, which also showed that the electron accepting capabilities of quinones can be increased by Lewis acid complexation to facilitate SET. Hence, this study provides proof of principle for the use of transient radical ion pairs for selective C–H bond activation processes. Currently, we are exploring the steric and electronic tuning of electron donor–acceptor complexes to enable the C–H bond activation of external substrates by *in situ* generated radical ion pairs.

Acknowledgements

This work was financially supported by the Deutscher Akademischer Austauschdienst (German Academic Exchange Service, DAAD) with a postdoc fellowship (C.H.), the Netherlands Organization for Scientific Research (NWO) by an ENW PPS LIFT grant (ENPPS.LIFT.019.009; J.C.S.), a VICI grant (VI.C.202.071; J.C.S.), and Shell Global Solutions International BV.

Conflict of Interest

The authors declare no conflict of interest.

Data Availability Statement

The data that support the findings of this study are available in the supplementary material of this article.

Keywords: C–H Activation · Frustrated Lewis Pairs · Radical-Ion-Pair · Radicals · Single-Electron Transfer

[1] a) D. W. Stephan, G. Erker, *Angew. Chem. Int. Ed.* **2010**, *49*, 46–76; b) D. W. Stephan, *Acc. Chem. Res.* **2015**, *48*, 306–316; c) D. W. Stephan, *J. Am. Chem. Soc.* **2015**, *137*, 10018–10032; d) D. W. Stephan, *Science* **2016**, *354*, aaf7229; e) J. Paradies, *Coord. Chem. Rev.* **2019**, *380*, 170–183; f) A. R. Jupp, D. W. Stephan, *Trends Chem.* **2019**, *1*, 35–48.

[2] a) J. Paradies, *Eur. J. Inorg. Chem.* **2019**, 283–294; b) A. R. Jupp, *Dalton Trans.* **2022**, *51*, 10681–10689.

[3] a) L. L. Liu, D. W. Stephan, *Chem. Soc. Rev.* **2019**, *48*, 3454–3463; b) A. Dasgupta, E. Richards, R. L. Melen, *Angew. Chem. Int. Ed.* **2021**, *60*, 53–65; c) L. L. Liu, L. L. Cao, Y. Shao, G. Ménard, D. W. Stephan, *Chem* **2017**, *3*, 259–267; d) L. L. Liu, L. L. Cao, D. Zhu, J. Zhou, D. W. Stephan, *Chem. Commun.* **2018**, *54*, 7431–7434; e) A. Merk, H. Großekappenberg, M. Schmidtmann, M.-P. Luecke, C. Lorent, M. Driess, M. Oestreich, H. F. T. Klare, T. Müller, *Angew. Chem. Int. Ed.* **2018**, *57*, 15267–15271; f) Y. Soltani, A. Dasgupta, T. A. Grazis, D. M. C. Ould, E. Richards, B. Slater, K. Stefkova, V. Y. Vladimirov, L. C. Wilkins, D. Wilcox, R. L. Melen, *Cell Rep. Phys. Sci.* **2020**, *1*, 100016; g) Y. Aramaki, N. Imaizumi, M. Hotta, J. Kumagi, T. Ooi, *Chem. Sci.* **2020**, *11*, 4305–4311; h) A. Dasgupta, K. Stefkova, R. Babaahmadi, B. F. Yates, N. J. Buurma, A. Ariafard, E. Richards, R. L. Melen, *J. Am. Chem. Soc.* **2021**, *143*, 4451–4464; i) L. J. C. van der Zee, S. Pahar, E. Richards, R. L. Melen, J. C. Slootweg, *Chem. Rev.* **2023**,*123*, 9653–9675; j) M. Ju, Z. Lu, L. F. T. Novaes, J. I. Martinez Alvarado, S. Lin, *J. Am. Chem. Soc.* **2023**, *145*, 19478–19489.

[4] a) G. Ménard, D. W. Stephan, *Angew. Chem. Int. Ed.* **2012**, *51*, 4409–4412; b) M.-A. Légaré, M.-A. Courtemanche, É. Rochette, F.-G. Fontaine, *Science* **2015**, *349*, 513–516; c) M.-A. Légaré, É. Rochette, J. Légaré-Lavergne, N. Bouchard, F.-G. Fontaine, *Chem. Commun.* **2016**, *52*, 5378–5390; d) K. Chernichenko, M. Lindqvist, B. Kótai, M. Nieger, K. Sorochkina, I. Pápai, T. Repo, *J. Am. Chem. Soc.* **2016**, *138*, 4860–4868; e) É. Rochette, M.-A. Courtemanche, F.-G. Fontaine, *Chem. Eur. J.* **2017**, *23*, 3567–3571.

[5] G. Ménard, J. A. Hatnean, H. J. Cowley, A. L. Lough, J. M. Rawson, D. W. Stephan, *J. Am. Chem. Soc.* **2013**, *135*, 6446–6449.

[6] No stable optimized structure of $[N_2O\text{–}(Al(C_6F_5)_3)_2]^{\bullet-}$ could be found due to immediate N_2 liberation. The EA was thus approximated from an optimized structure with a fixed O–N bond length. However, this likely underestimates the actual EA (see Supporting Information for further details).

[7] Y. Liu, E. Solari, R. Scopelliti, F. Fadaei-Tirani, K. Severin, *Chem. Eur. J.* **2018**, *24*, 18809–18815.

[8] L. L. Cao, J. Zhou, Z.-W. Qu, D. W. Stephan, *Angew. Chem. Int. Ed.* **2019**, *58*, 18487–18491.

[9] During the preparation of this manuscript, a study on the regioselective aliphatic C–H functionalization by neutral radical pairs was published, see: Z. Lu, M. Ju, Y. Wang, J. M. Meinhardt, J. I. Martinez Alvarado, E. Villemure, J. A. Terrett, S. Lin, *Nature* **2023**, *619*, 514–520.

[10] a) Z. Dong, C. Pezzato, A. Sienkiewicz, R. Scopelliti, F. Fadaei-Tirani, K. Severin, *Chem. Sci.* **2020**, *11*, 7615–7618; b) H. Song, E. Lee, *Chem. Eur. J.* **2023**, *29*, 202203364; c) A. C. Shaikh, J. M. Veleta, J. Moutet, T. L. Gianetti, *Chem. Sci.* **2021**, *12*, 4841–4849.

[11] F. Holtrop, A. R. Jupp, N. P. van Leest, M. Paradiz Dominguez, R. M. Williams, A. M. Brouwer, B. de Bruin, A. W. Ehlers, J. C. Slootweg, *Chem. Eur. J.* **2020**, *26*, 9005–9011.

[12] F. Holtrop, A. R. Jupp, B. J. Kooij, N. P. van Leest, B. de Bruin, J. C. Slootweg, *Angew. Chem. Int. Ed.* **2020**, *59*, 22210–22216.

[13] Deposition numbers 2283471 (**1**), 2265214 (**2**), 2265212 (**3**), 2265213 (**4**), 2265210 (**5**), 2265209 (**6**), 2265211 (**7**), 2265220 (**8**) contain the supplementary crystallographic data for this paper. These data are provided free of charge by the joint Cambridge Crystallographic Data Centre and Fachinformationszentrum Karlsruhe Access Structures service.

[14] P. Rani, G. Rajput, R. A. Yadav, *Spectrochim. Acta Part A* **2015**, *137*, 1334–1347.
[15] a) J.-M. Lü, S. V. Rosokha, J. K. Kochi, *J. Am. Chem. Soc.* **2003**, *125*, 12161–12171; b) V. Ganesan, S. V. Rosokha, J. K. Kochi, *J. Am. Chem. Soc.* **2003**, *125*, 2559–2571; c) J. S. Miller, P. J. Krusic, D. A. Dixon, W. M. Reiff, J. H. Zhang, E. C. Anderson, A. J. Epstein, *J. Am. Chem. Soc.* **1986**, *108*, 4459–4466.
[16] a) S. Sasaki, K. Sutoh, F. Murakami, M. Yoshifuji, *J. Am. Chem. Soc.* **2002**, *124*, 14830–14831; b) M. Reißmann, A. Schäfer, S. Jung, T. Müller, *Organometallics* **2013**, *32*, 6736–6744.
[17] The C–O bond is of similar length as the ones in $PhCH_2DDQH$ (1.437(4) Å, 1.452(4) Å), see: V. S. Batista, R. H. Crabtree, S. J. Konezny, O. R. Luca, J. M. Praetorius, *New J. Chem.* **2012**, *36*, 1141–1144.
[18] X. Pan, X. Chen, T. Li, Y. Li, X. Wang, *J. Am. Chem. Soc.* **2013**, *135*, 3414–3417.
[19] R. T. Boeré, Y. Zhang, *Acta Crystallogr. Sect. C* **2013**, *69*, 1051–1054.
[20] a) X. Tao, C. G. Daniliuc, R. Knitsch, M. R. Hansen, H. Eckert, M. Lübbesmeyer, A. Studer, G. Kehr, G. Erker, *Chem. Sci.* **2018**, *9*, 8011–8018; b) B. L. Thompson, Z. M. Heiden, *Phys. Chem. Chem. Phys.* **2021**, *23*, 9822–9831; c) T. Imagawa, M. Nakamoto, R. Shang, Y. Adachi, J. Ohshita, N. Tsunoji, Y. Yamamoto, *Chem. Lett.* **2020**, *49*, 1022–1025; d) J. Wang, H. Cui, H. Ruan, Y. Zhao, Y. Zhao, L. Zhang, X. Wang, *J. Am. Chem. Soc.* **2022**, *144*, 7978–7982; e) S. Kong, S. Tang, T. Wang, Y. Zhao, Q. Sun, Y. Zhao, X. Wang, *CCS Chem.* **2023**, *5*, 334–340.

Manuscript received: September 9, 2023
Accepted manuscript online: October 13, 2023
Version of record online: October 26, 2023